

Interaction between the faces of a squat-type fatigue crack determined by use of the grating holographic interferometry

P. Pyrzanowski, J. Stupnicki

Institute of Aeronautics and Applied Mechanics,
Warsaw University of Technology, Poland

ABSTRACT:

The paper presents the results of experimental study of interaction between faces of a squat-type fatigue crack. The phenomenon of crack faces interaction plays an important role in prediction of the rail head crack development. The results indicate that the conditions of crack faces interaction vary along the crack length. The values of determined crack faces interaction factor will be used in a numerical simulation of fatigue crack development.

INTRODUCTION

The present work is devoted to the problem of fatigue crack propagation in rail raceways. Those cracks often called “squat” or “black spot” appeared in the 1980s in high-speed lines in Western Europe and Japan. In Poland cracks of that type appeared in the end of the XX century in the tracks in which ten years earlier the rails of higher strength properties, resistant to abrasive wear had been used. The commonly accepted form of a crack of the squat-type is presented in Figure 1.

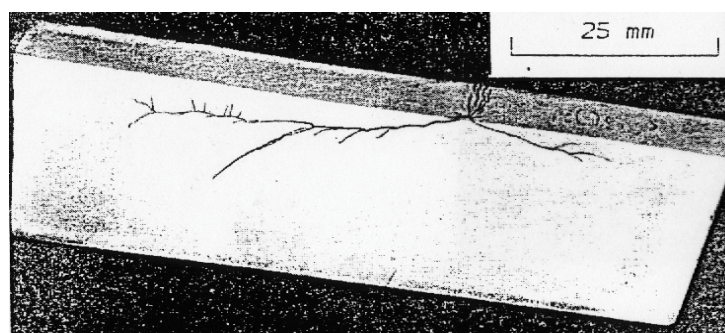


Figure 1: Crack of the “squat” type.

Two branches of a crack can be seen. The longer one with some branching follows the direction of rolling, while the shorter one takes the direction

opposite to the load motion. The crack propagating in the direction of motion often turns to a crack penetrating the whole rail.

The cracks observed in rails of Polish Railways have a slightly different form. Figure 2 shows a typical form of a large size singular crack, initiated on the rolling strip.

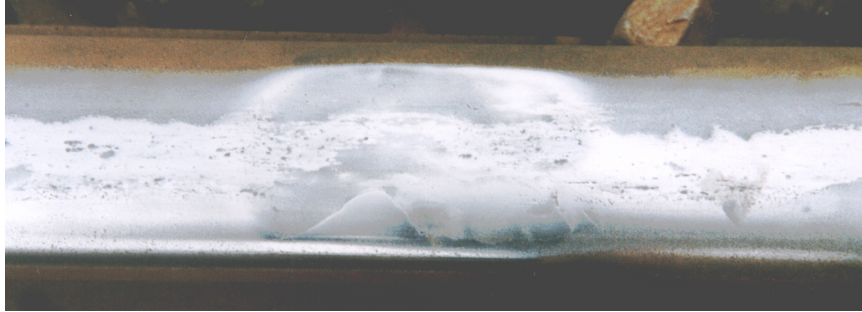


Figure 2: Photo of a squat-type crack appearing in rails in Poland.

In many works propagation of a crack of the squat-type was modeled, e.g., [1-5], however, some problems still need attention and detailed explanation.

Paper [6] is devoted to numerical simulation of crack of the squat-type. The analysis was focused on seeking parameters which affect most strongly the values and amplitudes of Stress Intensity Factors (SIFs) at the crack tip during the wheel rolling process. A semi-elliptical squat-type of crack in a rail head was analysed taking into account the real shapes of wheel and rail, and interactions between the rail and wheel as well as between the crack faces due to a moving load. The crack size, normal and traction loads, residual stresses as well as stresses due to bending of the rail and rail temperature variation were investigated. The study proved that many factors contribute to the stress state at a tip of the crack and affect the Stress Intensity Factors. But the most significant and most uncertain ones are the interactions between the crack faces, which manifest through the value of friction coefficient between the crack faces. Hence, a more accurate description of the process of crack faces interaction is necessary.

Further investigations were conducted using 2D models, in which different ways of representation of the fatigue crack interaction were examined in detail [7, 8]. To the 2D model of the rolling process of a cylinder along a raceway with a crack, the conditions of crack faces interaction presented in Figure 3 were introduced.

Paper [9] presents the discussion of two models of crack faces interaction, namely with the crack faces covered with layers of a worn out

material, the properties of which were determined basing on the results of experiments and with the crack faces covered with micro-asperity, which force a crack dilatation accompanying the tangential displacements.

All the above mention models used in numerical simulations allow for drawing the conclusions that more realistic representation of interaction between the crack faces is strongly needed.

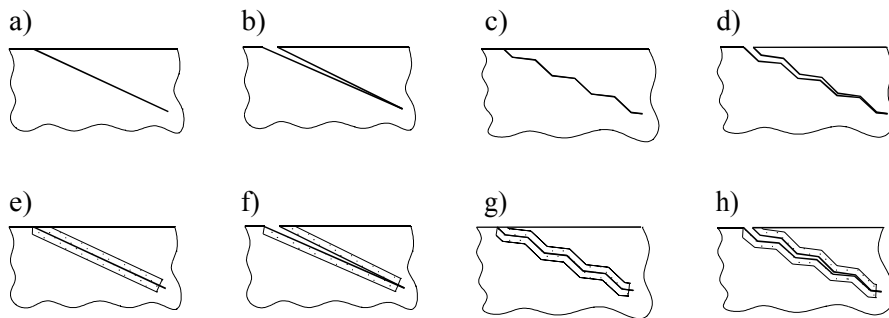


Figure 3: Conditions of the crack faces interaction. The surface braking crack with the faces: a) flat, b) flat with a gap between them, c) with a saw-like tortuosity, d) with a saw-like tortuosity and a gap between them, e) flat with layers of a material of deteriorated properties, f) flat with layers of a material of deteriorated properties, and a gap between them, g) with a saw-like tortuosity and with layers of a material of deteriorated properties, h) with a saw-like tortuosity, layers of a material of deteriorated properties and with a gap between them

EXPERIMENTAL INVESTIGATION OF CRACK THE FACES INTERACTION UNDER NORMAL AND TANGENTIAL LOADS

An experimental study using the Grating Holographic Interferometry (GHI) has been carried out which allows for determination of full field displacement vector components in the crack-adjacent zone and the interaction between the crack face asperity [10-12].

The examined object

The samples were produced of the slices cut out from the rail heads in which after 12 years of exploitation the squat-type of crack were detected. Figure 4a shows a section of a railhead with a crack and Figure 4b shows

a cube cut out from the rail head with a squat-type crack. The cube was selected from many others cut out from the rails, because the investigated crack should be relatively plain and perpendicular to the front surface of the sample. Then the selected cube was welded by use of a laser beam to console, which could be mounted to the clamping grips (Figure 5). The front surface of the sample was then ground and cross-line diffraction grating of a spatial frequency of 1200 line/mm was applied (Figure 4d).

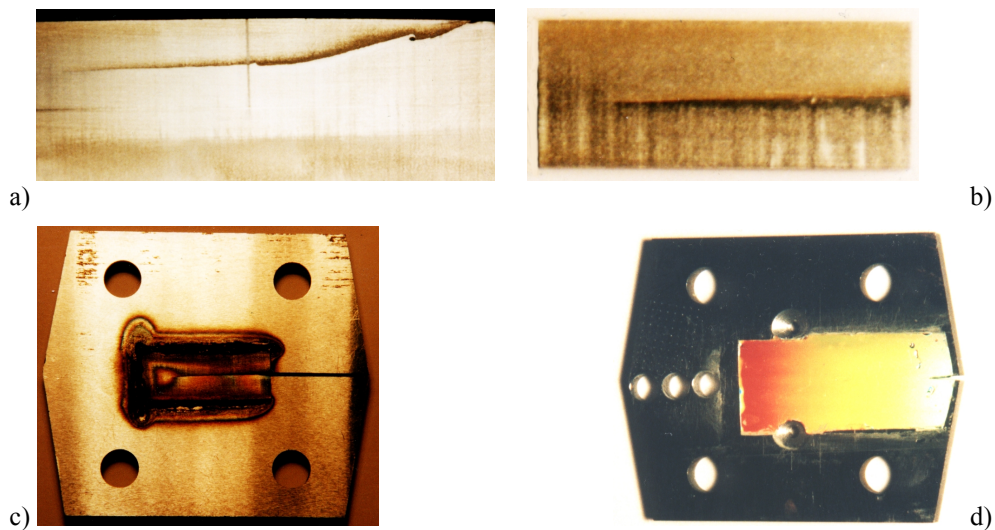


Figure 4: a) Section of the rail head with a crack, b) cube cut out from the rail-head, c) a cube welded to the sample, d) specimen with a grating

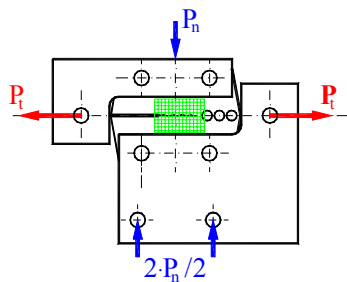


Figure 5: Sample with loading grips

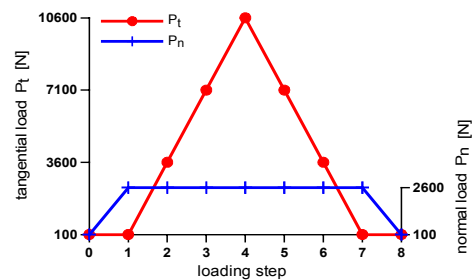


Figure 6: Scheme of the step-wise increase of P_t and P_n loads

The sample with the console was subject to the normal P_n and tangential P_t forces, respectively, to a crack plane. The forces were step-wise increased within the range from $P_0 \approx 0$ to $P_{max} = 10.5 \text{ kN}$, following the schemes presented in Figure 6, and the displacement distribution around the crack was registered at each step.

Figure 7, 8 present the sets of four interferograms, each reconstructed from single holographic plate, for normal and tangential loads, respectively.

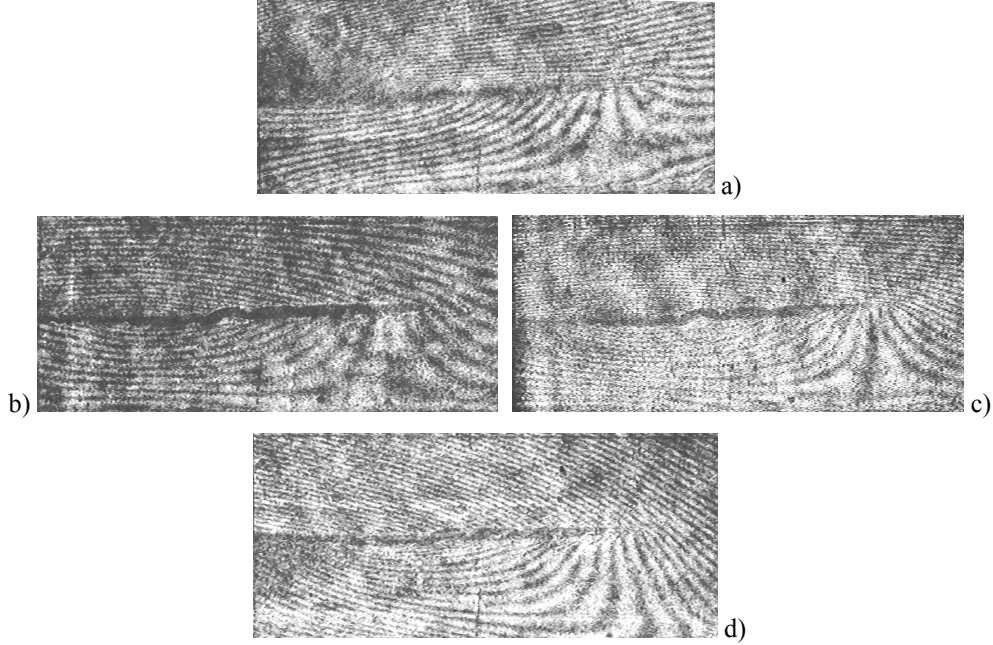


Figure 7: Set of interferograms for the normal load increase $\Delta P_n = 2600\text{ N}$ at $P_t = 0$, a) image of N_{1y} fringes, b) image of N_{2x} fringes, c) image of N_{1x} fringes, d) image of N_{2y} fringes

Using two of the four interferograms the components of displacement vector were determined from Eqs (1) and (2), which were derived in [6]. The interferograms a) and d) presented in Figure 6 or 7 were employed in the determination of v and w_1 components in the plane zy according to Eqs (1), while the interferograms b) and c) were used for the determination of components u and w_2 in the plane zx using Eqs (2).

By comparing the values of the components w_1 and w_2 normal to the sample surface calculated from two different sets of interferograms one can check the measurement accuracy and verify the fringe order accepted.

$$w_1 = \frac{\lambda}{2(1 + \cos\theta)} (N_{1y} + N_{2y}); \quad v = \frac{\lambda}{2\sin\theta} (N_{1y} - N_{2y}) \quad (1)$$

$$w_2 = \frac{\lambda}{2(1 + \cos\theta)} (N_{1x} + N_{2x}); \quad u = \frac{\lambda}{2\sin\theta} (N_{1x} - N_{2x}) \quad (2)$$

where N_{1y} , N_{2y} and N_{1x} , N_{2x} - fringe orders at the considered point on the interferograms a), b), c) and d), respectively.

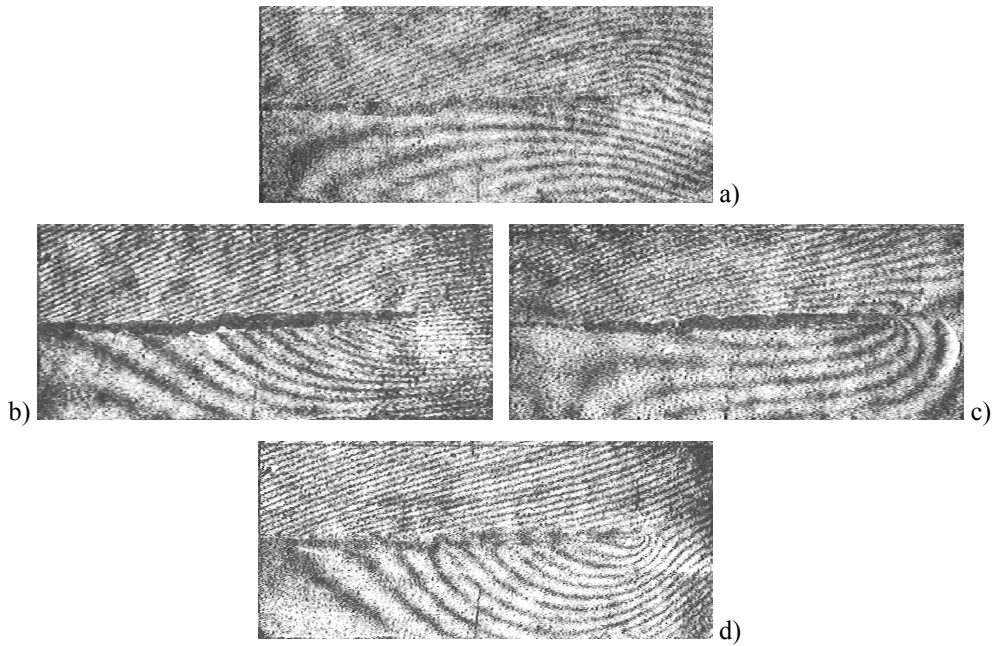


Figure 8: The set of interferograms for the tangential load increase $\Delta P_t = 3500N$ at $P_n = 2600 N = \text{const}$. a) image of N_{1y} fringes, b) image of N_{2x} fringes, c) image of N_{1x} fringes, d) image of N_{2y} fringes

The two dimensional maps of the in plane displacement vector components u, v (in μm) of sample surface for the normal load increasing step $\Delta P_n = 2600N$, at $P_t = 0 = \text{const}$ are shown in Figure 9 and for the tangential load increasing step equal to $\Delta P_t = 3500N$, at $P_n = 2600 N = \text{const}$ are shown in the Figure 10.

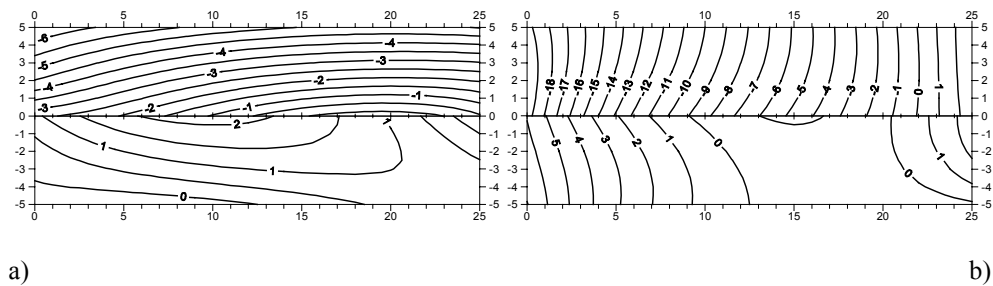


Figure 9: Contour maps of the a) u , b) v , in-plane displacement vector components at points of the sample surface for the normal load increase step $\Delta P_n = 2600N$, at $P_t = 0 = \text{const}$.

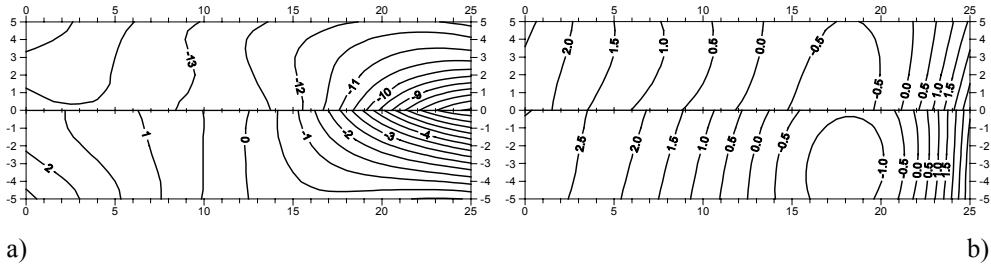


Figure 10: Contour maps of the a) u , b) v , in-plane displacement vector components at points of the sample surface for the tangential load increase step $\Delta P_t = 3500N$, at $P_n = 2600 N = const$.

RESULTS

Difference between the displacement vector components at the points located above and beneath the crack plane represent the crack opening (closing) Δv_s and micro-slip Δu_s on the crack faces. Figure 11a and 11b present these values for the first step of normal load increasing and the second step of tangential load increasing, respectively. In the diagrams the uncertainties of components of displacement vector evaluated as $\pm 0.2 \mu m$ are indicated.

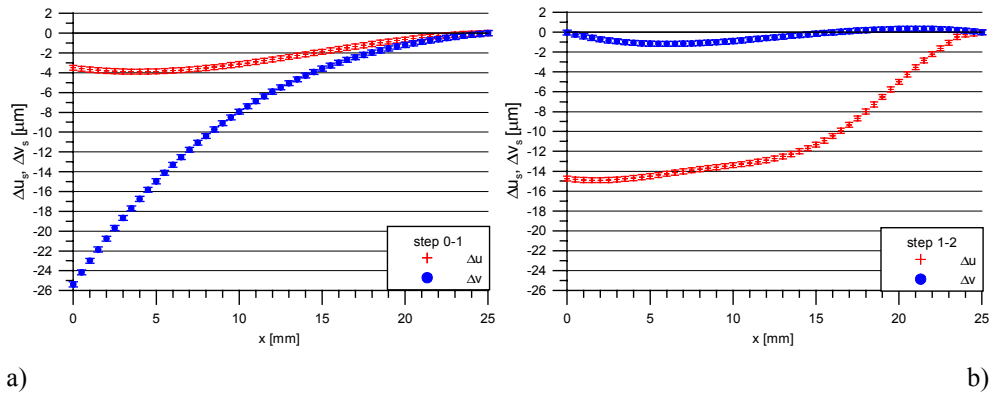


Figure 11: Diagrams of the crack closing Δv_s and the micro-slip Δu_s for the:
a) first step of load increasing $\Delta P_n = 2600N$, at $P_t = 0 = const$.
b) second step of load increasing $\Delta P_t = 3500N$, at $P_n = 2600N = const$

Basing on the values of the displacement vector components at the points located along the borders of the measurement area above the crack, the stress tensor components were determined by means of FEM, (assuming that the material remained elastic). That means that the crack faces interaction was determined, since the crack faces interaction corresponds to the stress tensor components S_{yy} normal to the crack and S_{xy} tangential to the crack plane (i.e. shear stress). Figure 12a and 12b present the aforementioned stress components for the consecutive steps of load increasing.

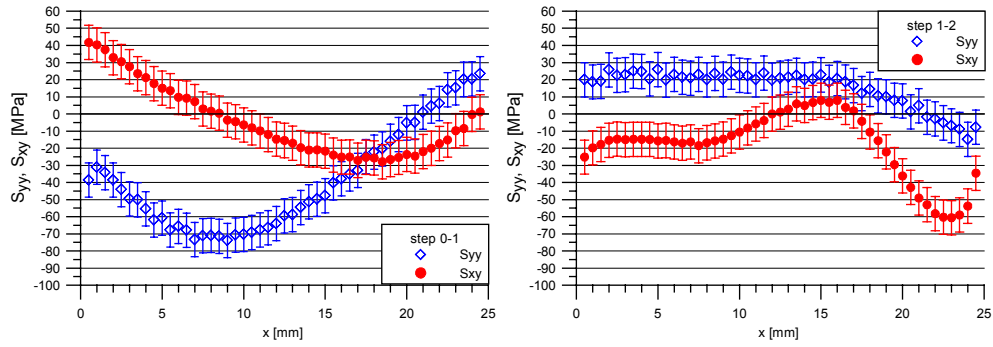


Figure 12: Stress tensor components S_{yy} normal to the crack and S_{xy} tangential to the crack plane (i.e. shear stress) along the crack faces for the
a) first step of load increase $\Delta P_n = 2600N$, at $P_t = 0 = const.$
b) second step of load increase $\Delta P_t = 3500N$, at $P_n = 2600N = const.$

Figure 13 presents the diagrams of total stress tensor components after two steps of load increasing i.e. the first step for normal load $\Delta P_n = 2600N$ and the second step for tangential load $\Delta P_t = 3500N$.

The presence of micro-slip during the second step of load increasing proves that the total magnitude of tangential stress tensor ΣS_{xy} reaches its limit for the current total normal stress component ΣS_{yy} , hence the value of resistance coefficient at a given point of crack face can be determined as:

$$f = \Sigma S_{xy} / \Sigma S_{yy} \quad (3)$$

The diagram of the factor f for the investigated squat-type of crack, along the crack length is presented in Figure 14. Its value is relatively small on prevailing length of the crack and reach high value at the tip of the crack.

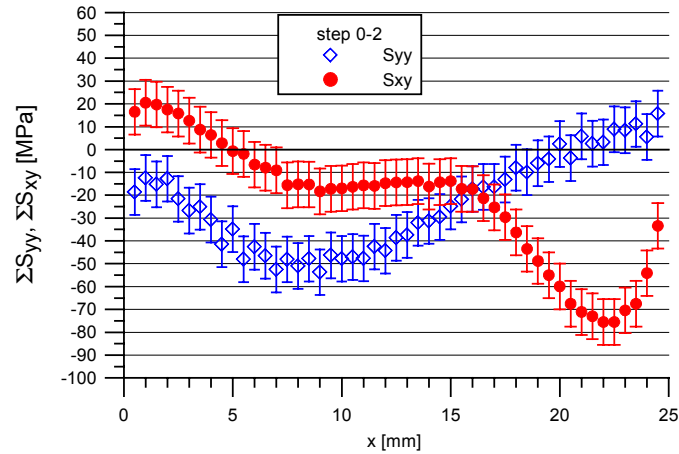


Figure 13: Total stress tensor component ΣS_{yy} normal and ΣS_{xy} tangential to the crack plane, respectively, along the crack faces (x) after the two steps of load increasing $\Delta P_n = 2600N$ and $\Delta P_t = 3500N$.

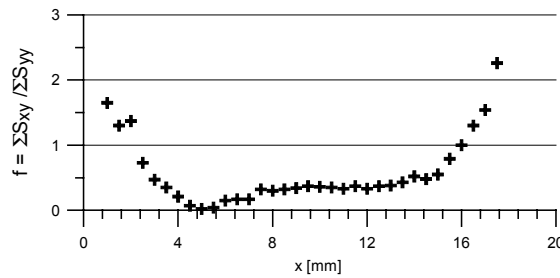


Figure 15: Diagram of the factor f versus of length of the crack

CONCLUSIONS

The method of Grating Holographic Interferometry when employed in measurements of displacement components allow the reliable results to be obtained.

- The displacement vector components u and v were obtained at points of the surfaces with the estimated accuracy $\delta u \approx \delta v \approx \pm 0.2 \mu m$.
- The GHI method allows for observation of the processes of crack opening or closing, crack faces micro-slips as well as crack dilatation in the courses of load increasing and decreasing, respectively.
- A continuous distribution of the displacement vector components at the border of the measurement area enables the determination of stress tensor components by use of FEM.

- The crack faces interaction determined in terms of the stress tensor components along the crack faces enables determination of the slip resistant factor f which varies substantially along the crack length for investigated sample with the crack cut out from the rail-head.
- The factor f determined on the basis of experimental results will be used in numerical simulation of rolling load applied to the raceway with the cracks.

REFERENCES

1. Bower, A.F. The influence of crack face friction and trapped fluid on surface initiated rolling contact fatigue cracks. ASME Journal of Tribology, 110, pp. 704-711, 1988.
2. Kaneta M., Murakami Y.: Propagation of semi-elliptical surface cracks in lubricated rolling/sliding elliptical contacts. J. of Tribology – vol.113, April 1991, pp. 270-275.
3. Duborg M.C., Kalker J.J.: Crack behavior under rolling contact fatigue, Rail quality and maintenance for modern railway operation. Kluwer Academic Publisher, 1993.
4. Olzak M., J.Stupnicki, R.Wójcik. Numerical analysis of 3D cracks propagating in the rail-wheel contact zone. Rail quality and maintenance for modern railway operation. By J.J.Kalker, D.F. Cannon, O.Orringer, Kluwer Acad. Publishers, pp. 385-395, 1993.
5. Kaneta M., Matsuda K., Murakami K, Nashikawa H.: A possible Mechanism for Rail Dark Spot Defects. Proc. of World Tribology Congress, London, September 1997.
6. Bogdański S., Olzak M., Stupnicki J.: Numerical Modelling of a 3D rail RCF “squat”-type crack under operating load. Fatigue & Fracture of Engineering Materials & Structures, 1998, pp. 923-935.
7. Olzak M., Stupnicki J.: Variations of the Stress Intensity Factors in the process of load rolling along a race containing a crack. Part I and II. Proc. of VII Conference on Fracture Mechanics, Kielce Cedzyna, 1999, pp. 109-123. (in polish)
8. Olzak M., Stupnicki J.: The influence of crack faces interaction model on the results of numerical study of stress intensity factors for the surface breaking cracks in race way. Int. Conf. on Contact Mechanics’99, Stuttgart, 1999.
9. Olzak M., Stupnicki J.: Numerical study of the Stress Intensity Factors for cracks in raceways with the experimentally determined interaction between crack faces. Conference on Contact Mechanics, Sevilla, 18-20 June 2001.
10. M. Szpakowska, P. Pyrzanowski, J. Stupnicki: Interference of fracture surfaces observed by means of optical methods for the cracks subjected to shear and compression. Proceedings of IUTAM Symposium Advanced Optical Methods and Application in Solid Mechanics, Poitiers, France, Sept/Oct. 1998.
11. Szpakowska M., Determination of rigidity of a layer coating a fatigue crack under normal and tangential loads acting simultaneously. PhD Thesis, Warsaw University of Technology, Warsaw 2000. (in polish)
12. P. Pyrzanowski, J. Stupnicki – Evaluation of Contact Rigidity of Fatigue Crack Faces for Numerical Models of RCF Crack Growth. Proceedings of GESA Symposium 2001 – VDI Berichte 1599, Chemnitz, Germany 2001 – pp. 353-361

ACKNOWLEDGEMENT: The work has been financially supported by the State Committee for Scientific Research under grant No. 8 T07A 012 20